

The small GTPase R-Ras regulates organization of actin and drives membrane protrusions through the activity of PLC ϵ

Aude S. Ada-Nguema¹, Harry Xenias², Jake M. Hofman³, Chris H. Wiggins⁴, Michael P. Sheetz² and Patricia J. Keely^{1,*}

¹Department of Pharmacology, University of Wisconsin-Madison, Madison, WI 53706, USA

²Department of Biological Sciences, Columbia University, New York, NY 10027, USA

³Department of Physics, Columbia University, New York, NY 10027, USA

⁴Department of Applied Physics and Applied Mathematics, Center for Computational Biology and Bioinformatics, Columbia University, New York, NY 10027, USA

*Author for correspondence (e-mail: pjkeely@wisc.edu)

Journal of Cell Science 119, 4364 (2006) doi:10.1242/jcs.03260

There was an error published in *J. Cell Sci.* **119**, 1307-1319.

The corresponding author regrets to have omitted, and wishes to properly acknowledge, Chris Wiggins and Jake Hofman for work presented in this paper.

Chris Wiggins (Applied Physics and Applied Mathematics Department, Columbia University) and Jake Hofman (graduate student in the Department of Physics, Columbia University) designed and developed several thousand original lines of code in the programming language MATLAB to produce the analysis program used in the data analysis shown in Fig. 1. Since their contribution was substantial, they should have been listed as co-authoring this work. The correct header of this article is shown above.

Moreover, the reference in Fig. 1 that the methods used were those described by Giannone et al. (Giannone et al., 2004) is wrong. Instead, the analysis used the novel MATLAB program developed by C.H.W. and J.M.H.

The corresponding author apologizes for these errors.

The small GTPase R-Ras regulates organization of actin and drives membrane protrusions through the activity of PLC ϵ

Aude S. Ada-Nguema¹, Harry Xenias², Michael P. Sheetz² and Patricia J. Keely^{1,*}

¹Department of Pharmacology, University of Wisconsin-Madison, Madison, WI 53706, USA

²Department of Biological Sciences, Columbia University, New York, NY 10027, USA

*Author for correspondence (e-mail: pikeely@wisc.edu)

Accepted 13 December 2005

Journal of Cell Science 119, 1307-1319 Published by The Company of Biologists 2006
doi:10.1242/jcs.02835

Summary

R-Ras, an atypical member of the Ras subfamily of small GTPases, enhances integrin-mediated adhesion and signaling through a poorly understood mechanism. Dynamic analysis of cell spreading by total internal reflection fluorescence (TIRF) microscopy demonstrated that active R-Ras lengthened the duration of initial membrane protrusion, and promoted the formation of a ruffling lamellipod, rich in branched actin structures and devoid of filopodia. By contrast, dominant-negative R-Ras enhanced filopodia formation. Moreover, RNA interference (RNAi) approaches demonstrated that endogenous R-Ras contributed to cell spreading. These observations suggest that R-Ras regulates membrane protrusions through organization of the actin cytoskeleton. Our results suggest that phospholipase C ϵ (PLC ϵ) is a novel R-Ras effector mediating the effects of R-Ras on the actin cytoskeleton and

membrane protrusion, because R-Ras was co-precipitated with PLC ϵ and increased its activity. Knockdown of PLC ϵ with siRNA reduced the formation of the ruffling lamellipod in R-Ras cells. Consistent with this pathway, inhibitors of PLC activity, or chelating intracellular Ca²⁺ abolished the ability of R-Ras to promote membrane protrusions and spreading. Overall, these data suggest that R-Ras signaling regulates the organization of the actin cytoskeleton to sustain membrane protrusion through the activity of PLC ϵ .

Supplementary material available online at
<http://jcs.biologists.org/cgi/content/full/119/7/1307/DC1>

Key words: R-Ras, Integrin, PLC, Ca²⁺, Actin, Cell spreading, Cell adhesion

Introduction

Cell adhesion to the extracellular matrix is a complex phenomenon that occurs in stages. Adhesion starts with the interaction of integrins with the extracellular matrix (ECM), followed by active cell spreading and culminates in the contraction of the actomyosin cytoskeleton. Following contact with the ECM, cells dynamically remodel the actin cytoskeleton (Jones et al., 1998; van Kooyk and Figdor, 2000; van Kooyk et al., 1999), which drives membrane extension during cell spreading (Chen et al., 2003; Engler et al., 2004; Wakatsuki et al., 2001) and continues until the cell has reached its maximum contact area with the substratum. Cells spread by multiple mechanisms, in part dominated by either lamellipodia- or filopodia-based membrane extensions, depending on the cell type, fate and environment. Most of the events involved in the structural regulation of membrane protrusions have been well characterized (Pantaloni et al., 2001; Pollard and Borisy, 2003; Small et al., 2002). Lamellipodia are composed of short actin filaments that are highly branched owing to the activity of capping and severing proteins (Pollard and Borisy, 2003; Small et al., 2002). Filopodia are composed of long, unbranched, parallel bundles of actin filaments and require a decrease in capping and severing protein activity and the anti-capping activity of Mena/VASP (Bear et al., 2002; Mejillano et al., 2004; Svitkina

et al., 2003). Although the actin-binding proteins regulating lamellipodial and filopodial protrusions have been well studied, much less is known about the upstream signaling pathways that regulate these events.

Initiation of cell adhesion and spreading requires an increase in cytosolic Ca²⁺ concentration [Ca²⁺]_i (Pettit and Hallett, 1996a; Pettit and Hallett, 1996b; Pettit and Hallett, 1998; van Kooyk and Figdor, 2000). The Ca²⁺ rise is mediated through the release of intracellular Ca²⁺ stores by inositol triphosphate (IP₃) produced as a result of the activity of phospholipase C (PLC); as well as an influx of extracellular Ca²⁺ through Ca²⁺ channels at the plasma membrane (McNamee et al., 1993; McNamee et al., 1996). The activation of PLC has been shown to initiate cell spreading in multiple cell types (Jones et al., 2005; Pettit and Hallett, 1998), and initiates membrane protrusions during carcinoma cell migration (Mouneimne et al., 2004). These effects of PLC activity are potentially carried out in two ways. First, the mobilization of intracellular Ca²⁺ stores by IP₃ production can activate capping proteins (Arora et al., 2003; Arora et al., 2004; McGough et al., 2003). Second, by hydrolyzing phosphatidylinositol 4,5-bisphosphate (PIP₂), PLC also relieves the inhibitory effect of PIP₂ on capping and severing proteins (Sechi and Wehland, 2000; Takenawa and Itoh, 2001).

R-Ras, a member of the Ras subfamily of small GTPases,

promotes cell adhesion, integrin activation, spreading, migration, cell polarity, axonal outgrowth and phagocytosis (Berrier et al., 2000; Ivins et al., 2000; Jeong et al., 2005; Keely et al., 1999; Kwong, 2003; Self et al., 2001; Sethi et al., 1999; Wozniak et al., 2005; Zhang et al., 1996) through mechanisms not fully known. These cellular events require the tight regulation of actin dynamics, suggesting that R-Ras signaling contributes to the modulation of the actin cytoskeleton. Furthermore, many of these events are driven by persistent protrusions mediated by lamellipodia formation. We found that R-Ras activation drives persistent membrane protrusion and promotes cell spreading, whereas knockdown of endogenous R-Ras inhibits protrusion and spreading. Moreover, expression of constitutively active R-Ras changes the dynamics of membrane protrusion to a lamellipodium-based mode of spreading, whereas dominant-negative R-Ras enhances filopodial-based protrusions. This switch was associated with a longer protrusive process mediated by a strong ruffling lamellipod. The formation of the ruffling lamellipod was blocked by PLC inhibitors and by the Ca^{2+} chelator BAPTA. We find evidence that PLC ϵ is a novel R-Ras effector, as it coprecipitates with R-Ras and is activated by R-Ras. Furthermore, knockdown of PLC ϵ with siRNA inhibited the ability of R-Ras cells to form the ruffling lamellipod. Overall these data suggest that R-Ras activity sustains protrusive motility during cell spreading by regulating the actin cytoskeleton through the activity of PLC ϵ .

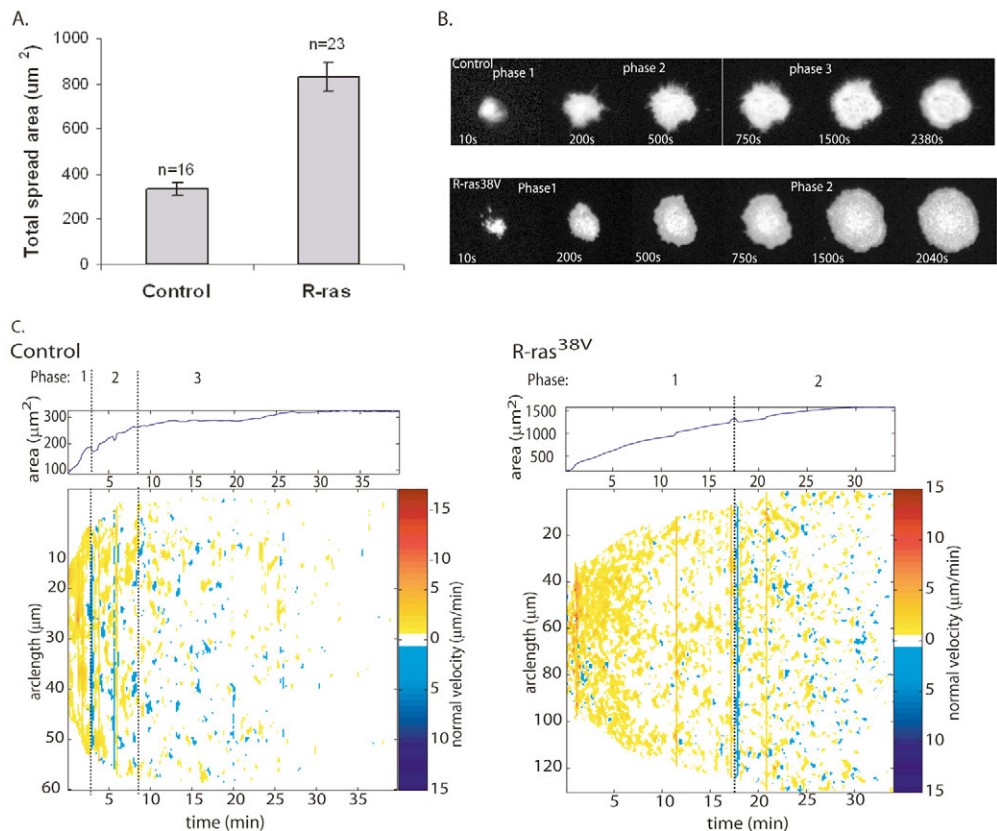
Fig. 1. Cells expressing constitutively activate R-Ras spread by continuously extending lamellipodia with few retraction events. (A) Total area of spread MCF10A cells comparing cells expressing vector alone with those expressing R-Ras^{38V}. Bar graph represents the average total spread area of 23 R-Ras cells or 16 control cells \pm s.e.m. Note that R-Ras-expressing cells are more than twice as spread as control cells. (B) TIRF images of an individual control and R-Ras^{38V}-expressing cell during spreading on 10 $\mu\text{g}/\text{ml}$ fibronectin. Brighter regions represent areas of greater contact with the ECM. (See Movies 1 and 2, in supplementary material.) (C) Analysis of protrusion and retraction events for control and R-Ras^{38V}-expressing cells. Images such as those shown in B were analyzed as described (Giannone et al., 2004) to characterize cell-edge dynamics. Top traces show the increase in total cell area over time for a representative control and R-Ras^{38V} cell. Radial edge velocity maps of the entire membrane periphery plotted as a function of time and arc length are shown below, where arc length denotes the separation between two polar coordinates along the periphery of the cell. Membrane activity was determined and expressed as the velocity of protrusion events (warm colors) or retraction events (cool colors). Dotted lines delineate the phases in cell spreading.

Results

R-Ras promotes spreading by inducing early continuous protrusive events

R-Ras potently enhances cell adhesion and subsequent events of adhesion-based signaling (Kwong, 2003; Zhang et al., 1996). To better understand mechanisms by which R-Ras increases cell adhesion, the immediate events that occur during initial ECM contact and spreading of cells were determined using total internal reflection fluorescence (TIRF) microscopy (Dubin-Thaler et al., 2004; Giannone et al., 2004). TIRF allowed us to study the dynamics of cell spreading at the region of contact between the cell and the extracellular matrix by exploiting the high contrast between contact and non-contact areas. Cell adhesion was induced by centrifugation and the kinetics of cell spreading were observed during the first 40 minutes of adhesion. MCF10A cells overexpressing constitutively active R-Ras (R-Ras^{38V}) spread to a greater extent than control cells. On average, control cells reached a maximum spread area of 350 μm^2 , whereas their R-Ras counterpart reached a spread area of 800 μm^2 during the same time period (Fig. 1A).

Differences in cell spreading kinetics could be explained by a switch in the mechanism of cell spreading when R-Ras was activated. In general, control cells spread by extending filopodia-like structures, with minimal protrusive activity as shown by the uniform intensity of TIRF images during cell spreading (Fig. 1B and Movie 1 in supplementary material).



This indicated that this cell was making stable contact with the ECM even as the contact area of the cell with the ECM was increasing (Fig. 1B). Contrary to filopodial extensions, R-Ras^{38V}-expressing cells had a smoother leading edge (Fig. 1B and Supplementary material Movie 2). Interestingly, R-Ras^{38V} cells had a stronger TIRF signal at the center of the cell surrounded by a lower intensity at the cell leading edge. Thus, unlike the cell center, the protrusive edge of these cells did not make strong contact with the ECM as the cell was spreading. The intensity became even after 500-700 seconds, suggesting that the cells protruded their leading edge for this period of time before they could stabilize these protrusions.

Subsequent mathematical analysis (Dubin-Thaler et al., 2004), of TIRF images demonstrated that control cells initiated spreading with a brief global burst (3 minutes) of protrusive activity. This was followed by alternating retractive and protrusive events (displayed in Fig. 1C as cool and warm colors, respectively) for the next 5-15 minutes and ended with a decline in membrane activity (>15 minutes). These protrusive stages correlated with the increase in cell surface area (Fig. 1C, top panel). The kinetics of cell spreading were altered in R-Ras^{38V}-expressing cells. The protrusive stage was longer, lasting about 15 minutes on average (Fig. 1C). The timing of this protrusive phase correlated with the time at which the leading edge of R-Ras cells had little interaction with the substratum as determined by TIRF. The second phase of spreading started with a decrease in the edge extension events and a burst in cell edge retraction events (phase 2; Fig. 1C). Strong contact with the ECM correlated with the appearance of retraction events at this time. Thus, the duration of the initial protrusive activity set the spreading behavior of the cell, and this duration was increased in cells expressing active R-Ras. In summary, TIRF analysis of membrane dynamics in R-Ras^{38V} cells indicates that the major difference in the spreading of control and R-Ras cells is defined by the duration of the initial protrusive events that lasted 3 minutes in control cells and 15 minutes in R-Ras cells.

R-Ras activation induces the formation of a strong ruffling lamellipod and inhibits filopodia

The observation that the duration of the initial protrusive events in R-Ras^{38V}-expressing cells is fivefold higher than control cells prompted us to investigate the underlying mechanism of that increase. Control and R-Ras cells were fixed and stained with TRITC-phalloidin to determine the structure of the actin cytoskeleton during cell spreading. Upon adhesion to collagen I or human fibronectin, control cells spread with a combination of filopodia and lamellipodia (Fig. 2A). These cells acquired a polarized phenotype within 45 minutes (data not shown). By contrast, cells expressing R-Ras^{38V}, spread faster and exhibited a prominent peripheral actin network reminiscent of thick lamellipodia or ruffles, referred to hereafter as a 'ruffling lamellipod' (Fig. 2A). At the end of spreading (>90 minutes), R-Ras^{38V} cells formed strong stress fibers and large focal adhesions, but did not acquire a polarized morphology (data not shown). To determine whether the effects of R-Ras on actin organization were specifically integrin dependent, cells were plated on poly-L-lysine (Bailly et al., 1998; Dubin-Thaler et al., 2004; Giannone et al., 2004). Here too, control and R-Ras^{38V} cells organized their actin cytoskeletons differently (Fig. 2A, bottom panels). Control cells formed extensive

filopodia upon adhesion, whereas cells expressing R-Ras^{38V} did not form filopodia, but had the same ruffling lamellipod. Thus activation of R-Ras changed the organization of the actin cytoskeleton in an integrin-independent manner. Contrary to activated R-Ras, expression of dominant-negative R-Ras^{41A} in MCF10A cells enhanced filopodia formation (arrows in Fig. 2B).

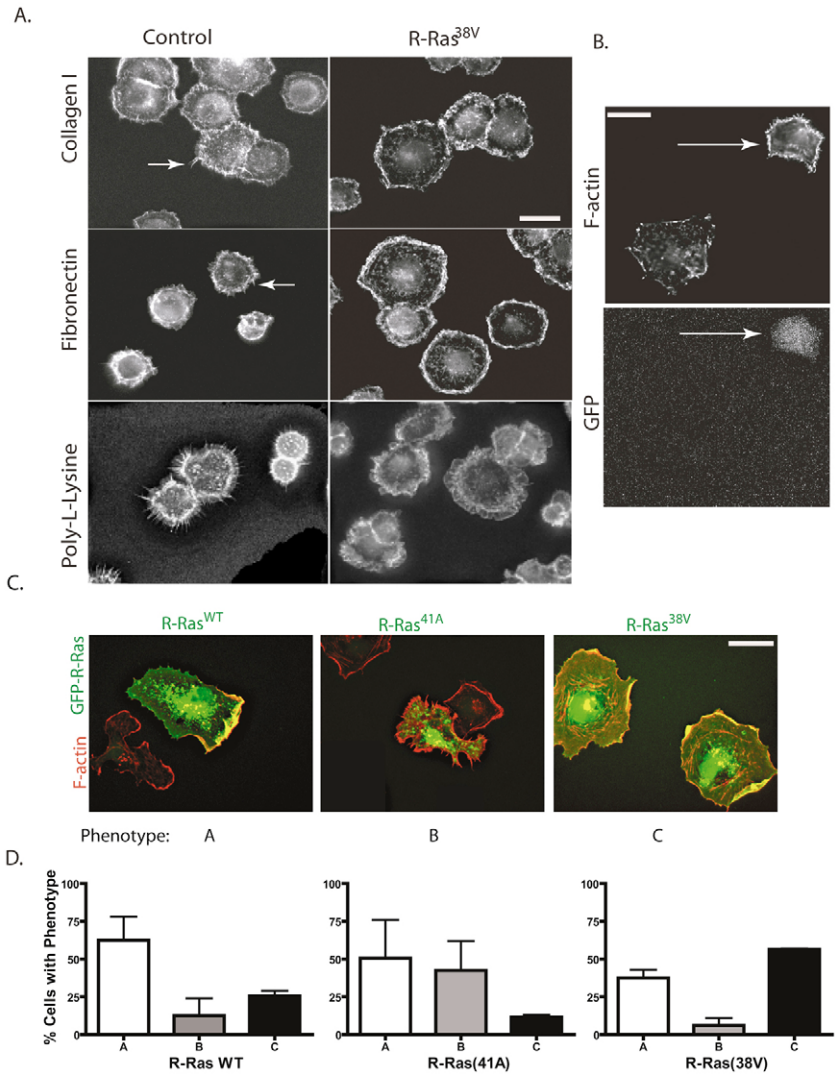
To further examine the role of R-Ras in the regulation of membrane protrusions, wild-type, dominant-negative and constitutively active GFP-R-Ras were transiently transfected into Cos7 cells, and spreading on fibronectin was determined. These cells were used in order to determine effects of R-Ras under transient transfection conditions, rather than the stable cell lines that are usually required for both MCF10A and T47D breast cells, which are not as readily transfected. Cells were double labeled with phalloidin to determine the localization of R-Ras relative to the actin cytoskeleton, and three phenotypes identified (A, B and C). Cells expressing GFP-R-Ras^{wt} often had polar membrane protrusions, and localized wild-type R-Ras to the protrusive leading edge (phenotype A, Fig. 2C,D). Consistent with results for MCF10A cells, GFP-R-Ras^{41A} enhanced the number of cells with prominent filopodia (phenotype B, Fig. 2C,D) and did not localize to the plasma membrane. By contrast, cells expressing GFP-R-Ras^{38V} often lost cell polarity and exhibited a strong ruffling lamellipod (phenotype C, Fig. 2C,D). Notably, like GFP-R-Ras^{wt}, GFP-R-Ras^{38V} localized to membrane ruffles. These observations strengthen our hypothesis that activation of R-Ras drives cell spreading by enhancing membrane protrusions that are lamellipodial-based. Moreover, these results suggest that R-Ras activity is a negative regulator of filopodial formation.

Previously, we reported that constitutive activation of R-Ras inhibited random cell migration of T47D breast epithelial cells by inhibiting cell polarity and membrane protrusion (Wozniak et al., 2005). To reconcile those results with the enhanced membrane protrusion and spreading resulting from R-Ras activation noted in Fig. 1, we determined whether expression of R-Ras^{38V} would affect the random migration of MCF10A cells. Control and R-Ras^{38V} cells were plated on fibronectin for 90 minutes and their ability to migrate was monitored by time-lapse video microscopy. Within that time frame, control cells actively migrated, whereas cells expressing R-Ras^{38V} showed greatly reduced migration (Movies 3 and 4 in supplementary material). Moreover, R-Ras cells had reduced ability to polarize front to rear, consistent with the lack of polarization also noted during cell spreading. Thus, consistent with our previous results in a different cell line, cells expressing active R-Ras^{38V} show impaired migration due in part to a defect in cell polarity (Wozniak et al., 2005). Overall, these data suggest that the mechanism by which R-Ras regulates membrane protrusions during spreading is distinct from the mechanism by which R-Ras modulates protrusions during migration.

Endogenous R-Ras contributes to cell spreading

To further determine whether endogenous R-Ras plays a role in cell spreading, MCF10A cells were transfected with siRNA directed against R-Ras, which caused a dramatic reduction in R-Ras expression levels (Fig. 3A). Knockdown of R-Ras caused a significant (>50%) decrease in the spreading of MCF10A cells, as determined by the spread cell area (Fig. 3B). Knockdown of R-Ras by RNAi in T47D cells also inhibited

Fig. 2. Expression of constitutively active or dominant-negative R-Ras regulates the organization of the peripheral actin network and formation of filopodia. (A) Stable expression of constitutively active R-Ras promotes a strong, branched peripheral actin network. MCF10A cells stably transfected with control vector or constitutively active R-Ras^{38V} were plated on collagen I (30 $\mu\text{g/ml}$), fibronectin (20 $\mu\text{g/ml}$) or poly-L-lysine (0.01%) for 30 minutes. The cells were then fixed and stained with TRITC-phalloidin to visualize F-actin. Note the dense peripheral actin and loss of filopodia in R-Ras^{38V}-expressing cells. A bubble is present in the lower right corner of control p-lysine cells. (B) Dominant-negative R-Ras enhances filopodia formation in MCF10A cells. MCF10A cells were transiently co-transfected with pCMV-R-Ras^{41A} and GFP to identify transfected cells. 48 hours post-transfection, the cells were assayed for their ability to spread on fibronectin-coated coverslips for 45 minutes. Arrow indicates a cell transfected with R-Ras^{41A}. (C) R-Ras regulates membrane protrusion and filopodia formation. Cos7 cells were transiently transfected with GFP:R-Ras^{WT}, GFP:R-Ras^{38V} or GFP:R-Ras^{41A}. 48 hours post-transfection, cells were detached and were allowed to adhere and spread on fibronectin (30 $\mu\text{g/ml}$) for 1 hour. Cells were then fixed and stained for F-actin. Overlay images of F-actin (red) and GFP-R-Ras (green) are shown. Note that GFP-R-Ras^{WT} localizes to leading edges, whereas GFP-R-Ras^{41A} is not found on the plasma membrane, and GFP-R-Ras^{38V} is localized more uniformly around the cells at the ruffling lamellipod. Representative phenotypes for each transfection are shown, and are labeled A, B and C. (D) Quantification of phenotypes shown in C. Note that expression of constitutively active R-Ras^{38V} dramatically enhances phenotype C, which has a strong peripheral actin network and no filopodia, whereas expression of dominant-negative R-Ras^{41A} promotes phenotype B, which has enhanced filopodia formation. Values represent the mean of three experiments \pm s.d. Bars, 10 μm (A-C).



cell spreading (not shown), consistent with previous results demonstrating knockdown of R-Ras by RNAi in these cells inhibited membrane protrusion and cell migration (Wozniak et al., 2005).

PLC pathways are required for the effect of R-Ras on cell spreading

The activation of PLC has been shown to initiate cell spreading and membrane protrusions in multiple cell types (Jones et al., 2005; Mouneimne et al., 2004; Pettit and Hallett, 1998). Based on the observations made in Figs 1-3, we hypothesized that the formation of the ruffling lamellipod in cells expressing R-Ras^{38V} was potentially mediated by the activation of PLC pathways. To test the role of PLC in R-Ras^{38V} signaling, cells were pretreated with U73122, a synthetic PLC inhibitor. Note that this is a broad-specificity PLC inhibitor, so it will not discriminate between PLC isoforms. Treatment of cells with 1 μM U73122 inhibited the ability of control cells to adhere and spread on fibronectin (Fig. 4A-C). In R-Ras^{38V} cells, the same concentration of U73122 had minimal effect on adhesion (Fig.

4A), but these cells could not spread well and more importantly, they could not form the ruffling lamellipod (Fig. 4B,C). However, 10 μM U73122 reduced adhesion of R-Ras-expressing cells to that of control cells (Fig. 4A). These data suggest that the formation of a ruffling lamellipod in R-Ras^{38V} cells is dependent on the activity of PLC.

PLC activity can potentially regulate protrusion via the activation of PKC downstream of DAG, and/or via the mobilization of intracellular Ca²⁺ that will regulate actin capping and severing proteins. Because cell spreading in epithelial cells is regulated by the mobilization of intracellular Ca²⁺ stores (Spoonster et al., 1997), and R-Ras activity has been linked to Ca²⁺ regulation (Koopman et al., 2003), we tested the effects of Ca²⁺ depletion on R-Ras-enhanced cell spreading. Cells in suspension were pretreated with 10 μM BAPTA-AM, a chelator of cytoplasmic Ca²⁺, for 20-30 minutes at 37°C. Treatment of both control and R-Ras^{38V} cells with BAPTA-AM inhibited cell adhesion to fibronectin (Fig. 4A). The inhibitory effect of BAPTA on cell adhesion could be lessened by reducing the incubation time, allowing us to assess

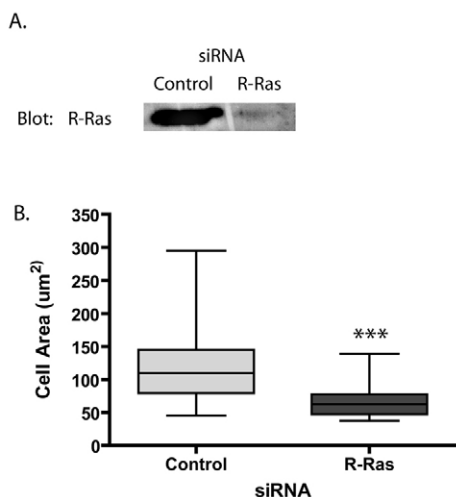


Fig. 3. Endogenous R-Ras contributes to cell spreading. MCF10A cells were transfected with siRNA oligonucleotides of a random sequence (control) or targeted against R-Ras. (A) siRNAs directed against R-Ras are effective. Half of the transfected cells were lysed, and equal cell numbers for control and R-Ras siRNA separated by SDS-PAGE. Transfers were immunoblotted with antibodies against R-Ras to demonstrate a significant knockdown with the anti-R-Ras siRNA. (B) Cell spreading is diminished by R-Ras knockdown. The other half of the cells transfected were detached and allowed to spread on 20 $\mu\text{g}/\text{ml}$ fibronectin for 45 minutes, fixed, and cell area was analyzed as described in the Materials and Methods using Image J software. Results for 20 cells are graphed in a box-and-whisker plot such that the horizontal line represents the mean, the box represents the 25% and 75% confidence intervals, and the error bars represent the s.d. *** $P < 0.001$ compared with cell area of control cells using a two-tailed unpaired t -test.

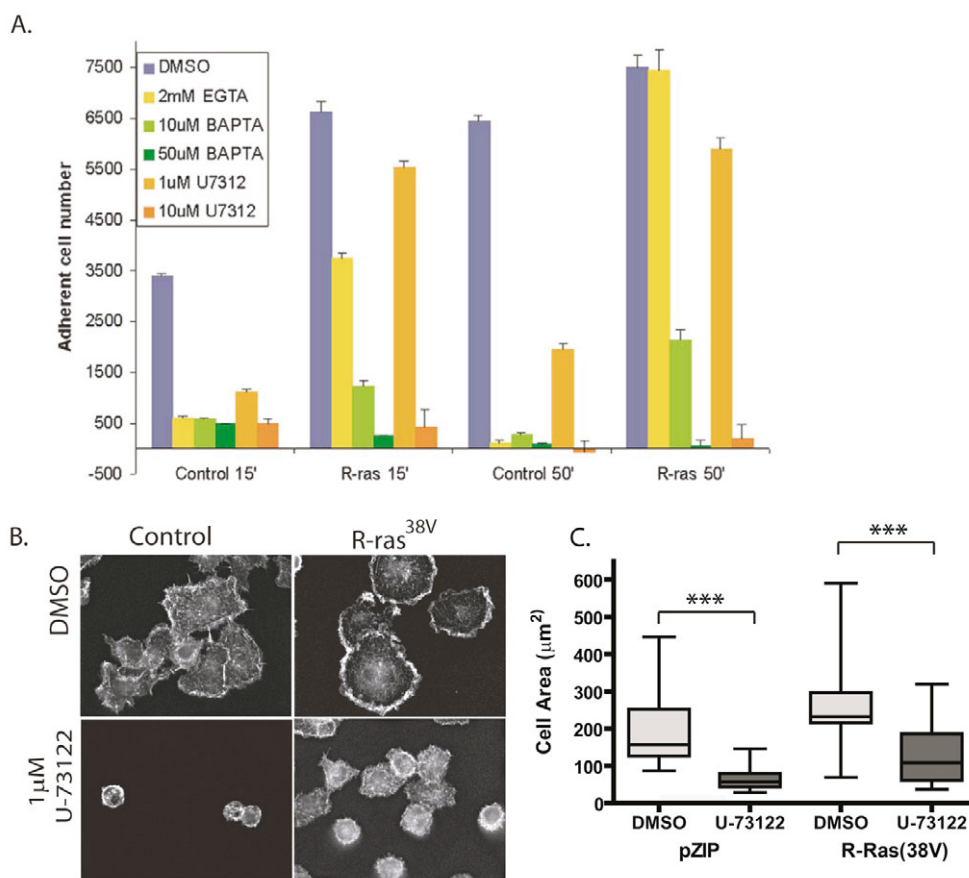
the effect of BAPTA-AM on cell spreading. BAPTA-AM inhibited the formation of the ruffling lamellipod in R-Ras cells and restored the formation of filopodia (Fig. 5A). Moreover, BAPTA-AM significantly diminished cell spreading (Fig. 5B). Since BAPTA-AM could inhibit adhesion (Fig. 4A), it was important to rule out effects on cell spreading that were secondary to adhesion; thus, cells were pre-plated on

fibronectin for 20 minutes before the addition of BAPTA-AM. Chelating intracellular Ca^{2+} after the initiation of cell spreading also abolished the ability of these cells to form the ruffling lamellipod (Fig. 5A) suggesting that cytoplasmic Ca^{2+} plays an important role in actin organization and cell spreading separate from mediating initial adhesion.

To verify that the effects of BAPTA-AM were specific to

Fig. 4. The formation of the ruffling lamellipod in R-Ras-expressing cells depends on PLC activity.

(A) Pharmacological inhibitors of intracellular Ca^{2+} and PLC inhibit R-Ras-enhanced adhesion. To assess adhesion, control and R-Ras^{38V}-expressing cells were loaded with 20 $\mu\text{g}/\text{ml}$ calcein-AM for 20 minutes. The cells were then pretreated with the indicated pharmacological agent (DMSO, EGTA, BAPTA or the broad-specificity PLC inhibitor, U73122) for 30 minutes, and allowed to adhere onto 96-well plates coated with 20 $\mu\text{g}/\text{ml}$ fibronectin for 15 and 50 minutes. The number of adherent cells was evaluated with a fluorescent plate reader, using a standard curve to determine cell number from calcein fluorescence. (B) Inhibition of phospholipase C reverts the strong peripheral actin ring induced by expression of R-Ras^{38V}. Control and R-Ras^{38V} cells were pretreated with 1 μM of the phospholipase C inhibitor, U73122, for 30 minutes followed by adhesion onto 20 $\mu\text{g}/\text{ml}$ fibronectin for 30 minutes. The cells were stained with Alexa-phalloidin to visualize F-actin. (C) Inhibition of phospholipase C diminishes cell spreading. The area of cells prepared as in B was analyzed with Image J, as in Fig. 3. Treatment of both control and R-Ras^{38V}-expressing cells with U73122 inhibits the measured area of cell spreading. Data represent measurements of >20 cells and are plotted as a box-and-whisker plots \pm s.d. *** $P < 0.001$.



intracellular, external Ca^{2+} was chelated by incubating cells with EGTA. Surprisingly, EGTA did not affect either lamellipod formation or spreading of R-Ras^{38V} cells (Fig. 5A). However, EGTA did inhibit adhesion of control cells and delayed the onset of adhesion in R-Ras cells (Fig. 4A). Because integrin-mediated adhesion is divalent cation-dependent, again cells were allowed to attach prior to treatment with EGTA to rule out effects on adhesion. Both pre-adherent control and R-Ras-expressing cells were unaffected by treatment with EGTA. Thus external Ca^{2+} is essential for the initiation of adhesion, but not for subsequent spreading, which is driven by cytosolic Ca^{2+} .

Chronic activation of PLC depletes internal Ca^{2+} stores

(Parekh, 2003). Because PLC may be activated downstream of R-Ras, we determined the ability of R-Ras^{38V} cells to mobilize internal Ca^{2+} stores. Control and R-Ras^{38V}-expressing cells were treated with thapsigargin (Tg), a selective inhibitor of the ER Ca^{2+} -ATPase (SERCA), which induces a transient flux in cytosolic Ca^{2+} concentration by preventing the active re-uptake of Ca^{2+} back into the continuously leaky ER lumen. When 4 μM thapsigargin was applied to control cells in suspension, a strong Ca^{2+} flux was observed (Fig. 5C). However, the same concentration of Tg had no effect on the Ca^{2+} concentration in R-Ras^{38V} cells (Fig. 5C) (Koopman et al., 2003). These experiments were repeated either in Ca^{2+} -free medium or with 1 mM calcium chloride, with the same results (data not shown).

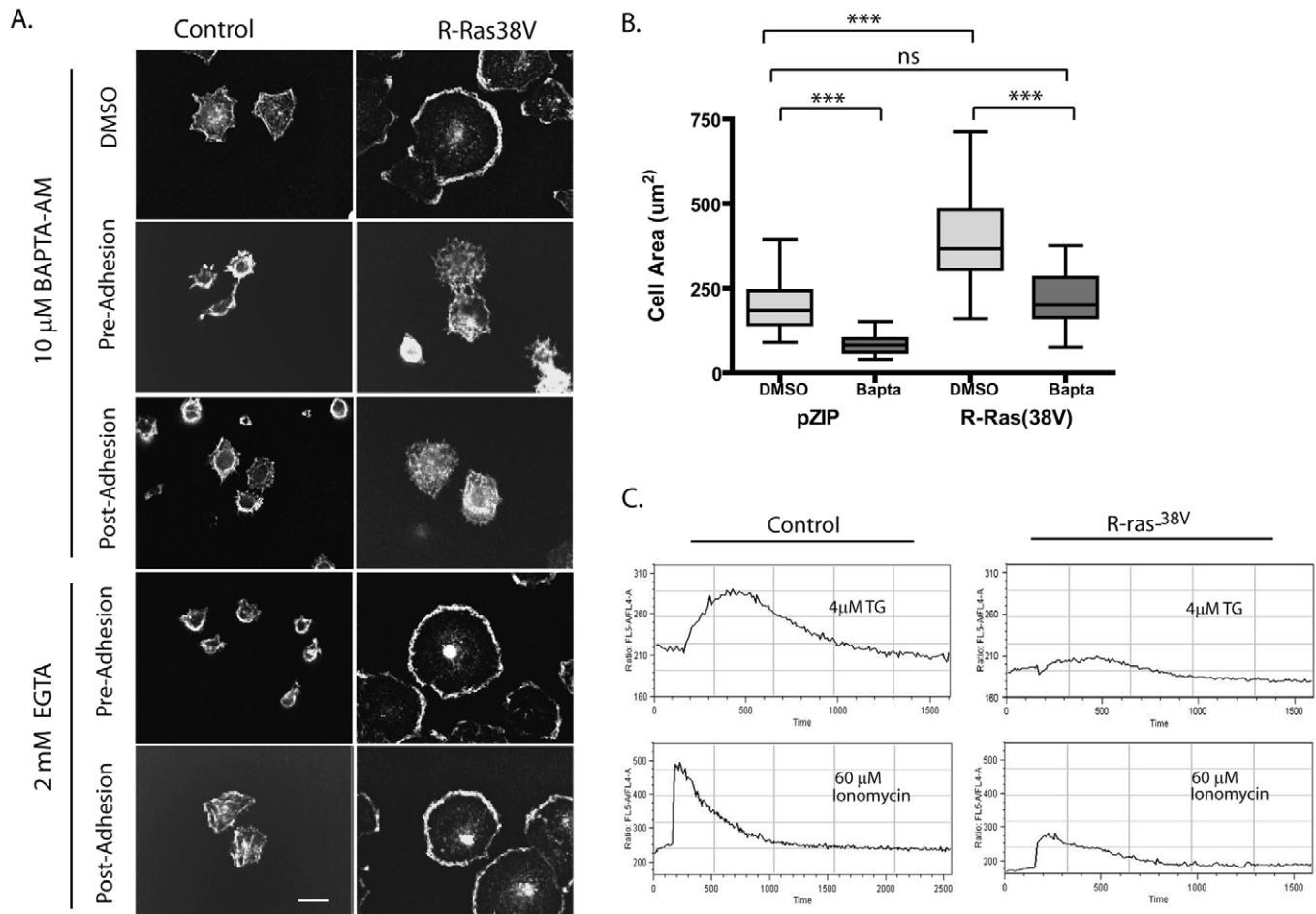


Fig. 5. Spreading and the strong peripheral actin ring induced by R-Ras is dependent on intracellular, but not extracellular Ca^{2+} . (A) The depletion of cytosolic Ca^{2+} , but not extracellular Ca^{2+} reduces the peripheral actin ring and rescues filopodia formation in R-Ras^{38V}-expressing cells. Control and R-Ras^{38V} cells were pretreated for 20 minutes with 10 μM BAPTA-AM for 20 minutes to chelate intracellular Ca^{2+} . The cells were then plated on 20 $\mu\text{g}/\text{ml}$ fibronectin-coated coverslips for 30 minutes in the presence of 10 μM BAPTA-AM (pre-adhesion) then fixed and stained for F-actin. Alternatively, untreated Control and R-Ras^{38V} cells were plated on 20 $\mu\text{g}/\text{ml}$ fibronectin until they were adherent followed by treatment with 10 μM BAPTA-AM for another 30 minutes (post-adhesion). To determine the role of external Ca^{2+} , cells were pretreated with 2 mM EGTA for 20 minutes and allowed to spread on 20 $\mu\text{g}/\text{ml}$ fibronectin (pre-adhesion), then fixed and stained for F-actin.

Alternatively, cells were allowed to adhere to fibronectin until they were adherent before the addition of 2 mM EGTA for another 30 minutes. Results are representative of three such experiments. Bar, 11 μm . (B) Chelation of intracellular Ca^{2+} reduces cell spreading. The spread area of more than 20 cells from the experiment shown in A was quantified and presented as described for Fig. 3. Treatment with BAPTA-AM significantly diminishes cell spreading in both control and R-Ras38V-expressing cells. *** $P < 0.001$; ns, not significant. (C) Endoplasmic reticulum Ca^{2+} stores are depleted in R-Ras cells. Control and R-Ras^{38V} cells were loaded with 20 $\mu\text{g}/\text{ml}$ of the Ca^{2+} indicator Indo-1-AM for 20 minutes at 37°C. The cells were then stimulated with 4 μM thapsigargin (TG) or 60 μM ionomycin for the duration of the measurement and Ca^{2+} flux was measured by flow cytometry. TG- and ionomycin-induced Ca^{2+} flux are diminished in cells expressing R-Ras^{38V}.

R-Ras^{38V}-expressing cells were largely unresponsive to every stimulus tested, including the Ca²⁺ ionophore, ionomycin (Fig. 5C), forskolin, bradykinin, 8-bromo-CPT-cAMP and db-cAMP (data not shown). These results suggest that chronic signaling due to expression of R-Ras^{38V} depletes internal Ca²⁺ stores, consistent with a model in which constitutive activation of R-Ras leads to over activation of PLC pathways and chronic release of Ca²⁺. Moreover, these results support the hypothesis that the mobilization of Ca²⁺ downstream of PLC activity is required for the initiation of cell spreading in breast epithelial cells and that R-Ras activation prolongs the activity of PLC in the initiation of cell protrusion.

R-Ras regulates phospholipase C ϵ

Phosphoinositide-specific phospholipases are a large family of enzymes that differ in structure and tissue distribution, but have the same function. In mammalian cells there are 11 PLC isozymes grouped in four different classes (PLC β , δ , ϵ and γ) that are regulated by distinct mechanisms. The function of PLC γ has been linked to integrin signaling (Keely and Parise, 1996). However, tyrosine phosphorylation of PLC γ was not

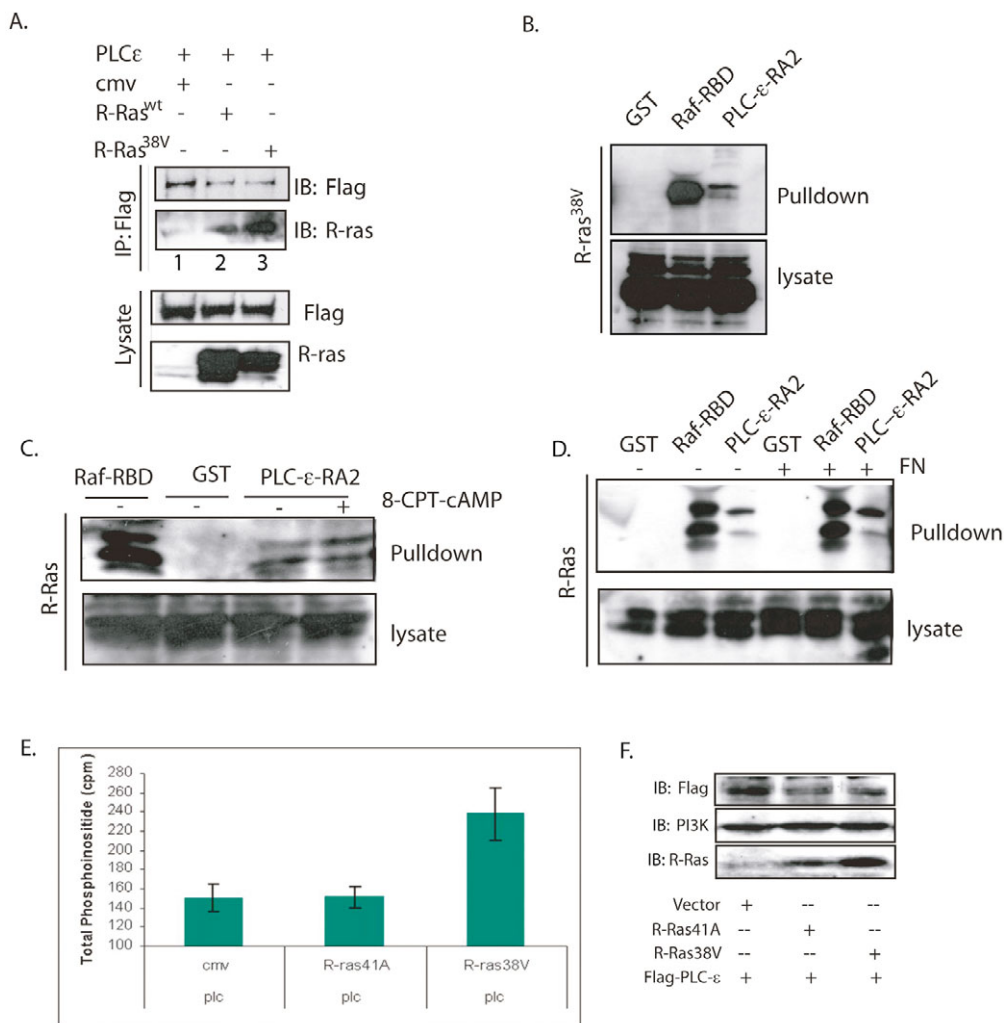
enhanced in cells expressing R-Ras^{38V}, suggesting that R-Ras does not activate PLC γ (data not shown).

PLC ϵ , the most recently cloned member of the PLC family, is activated by members of the Ras family of small GTPases and by increases in cytosolic Ca²⁺ concentration (Czyzyk et al., 2003; Kelley et al., 2001; Kelley et al., 2004; Song et al., 2001; Song et al., 2002). To investigate a link between R-Ras and PLC ϵ , their interaction in cells was evaluated. R-Ras^{WT} or R-Ras^{38V} was co-expressed with Flag-PLC ϵ in Cos7 cells, and PLC ϵ was immunoprecipitated with an anti-Flag antibody. We found that PLC ϵ co-immunoprecipitated R-Ras^{WT} and R-Ras^{38V} (Fig. 6A, lanes 2 and 3). These results suggest that PLC ϵ and R-Ras can interact in cells. Notably more R-Ras^{38V} was co-immunoprecipitated (Fig. 6A, lane 3), suggesting a preference for the active GTP-bound form of R-Ras.

GST-pulldown assays were used to investigate whether R-Ras interacts with the Ras-binding domain of PLC ϵ (RA2). R-Ras^{38V} expressed in MCF10A cells binds the RA2 domain of PLC ϵ (GST-PLC ϵ -RA2) (Fig. 6B). Endogenous R-Ras also bound to GST-PLC ϵ -RA2 (Fig. 6C,D). Activation of endogenous R-Ras, with 8-CPT-2Me-cAMP slightly enhanced

Fig. 6. R-Ras interacts with PLC ϵ .

(A) R-Ras co-immunoprecipitates with PLC ϵ in Cos7 cells. Cos7 cells were transfected with Flag-PLC ϵ and control vector (lane 1), R-Ras^{WT} (lane 2) or R-Ras^{38V} (lane 3), lysed and PLC ϵ immunoprecipitated with anti-Flag antibody. Association with R-Ras was determined by immunoblotting with anti-R-Ras antibody. (B-D) Active R-Ras interacts with the Ras-association domain, RA2, of PLC ϵ . A pull-down assay was performed by incubating GST-RA2 with lysates from MCF10A cells expressing-R-Ras^{38V} (B). Alternatively, lysates were obtained from control MCF10A cells that were stimulated with 8-CTP-2Me-cAMP for 30 minutes (C) or stimulated by adhesion to fibronectin for 45 minutes to activate endogenous R-Ras. In B-D, lysates were incubated with GST (negative control), GST-Raf-RDB (a robust, positive control), and PLC ϵ -RA2 domain for 2 hours at 4°C. Often endogenous R-Ras is noted as a doublet band, as seen here. (E) Constitutively active R-Ras activates PLC ϵ activity. Cos7 cells were transiently transfected with PLC ϵ and pCMV vector, pCMV-R-Ras^{41A} or pCMV-R-Ras^{38V} and a PLC activity assay was performed 48 hours post transfection. Data represent the means of two separate experiments each performed in duplicate. The minimum value of the y-axis is 100 cpm, which represents the background count. (F) Immunoblot for the PLC assay shown in E, demonstrating expression of Flag-PLC ϵ as well as R-Ras^{41A} and R-Ras^{38V} in transfected, unlabelled Cos7 cells.



binding to PLC ϵ -RA2 (Fig. 6C). However, activation of endogenous R-Ras with fibronectin did not significantly enhance binding to PLC ϵ -RA2 (Fig. 6D). Similar results were found for the Ras-binding domain of Raf, which robustly bound to endogenous R-Ras even in the absence of additional stimulation, suggesting that a pool of active R-Ras exists in cells.

The ability of R-Ras to activate PLC ϵ was determined with a PLC activity assay. Flag-PLC ϵ was co-expressed with either an empty pCMV5 vector (cmv), dominant-negative R-Ras^{41A}, or constitutively active R-Ras^{38V}. Forty-eight hours post-transfection, cells were assayed for PLC activity (Fig. 6E). Cells that were co-transfected with R-Ras^{38V} and PLC ϵ showed a high PLC activity when compared with cells that expressed either an empty vector or dominant-negative R-Ras (Fig. 6E). In this case, dominant-negative R-Ras did not further diminish the already low baseline PLC activity (Fig. 6E). Immunoblotting confirmed that these results were not due to expression differences, as we noted equal expression of R-Ras^{41A} or R-Ras^{38V} (Fig. 6F). Thus, activation of R-Ras enhances PLC ϵ activity in cells.

To further demonstrate that PLC ϵ is downstream of R-Ras signaling, PLC ϵ function was blocked using siRNA directed against PLC ϵ . PLC ϵ protein was knocked down to about 50% (Fig. 7A). In this cell population, there was a decrease in the mean area of spreading, with more cells having a smaller area (Fig. 7B). However, the difference was not statistically significant, perhaps reflecting that the knockdown was partial. Notably, knocking down PLC ϵ altered the actin cytoskeleton and the phenotype of the cells, and inhibited the formation of the large ruffling lamellipod during cell spreading (Fig. 7C, phenotype C). Although about 50% of R-Ras^{38V}-expressing cells were characterized by a strong ruffling lamellipod, this was inhibited to less than 5% upon treatment with PLC ϵ siRNA (phenotype C, Fig. 7D). Some cells treated with siRNA for PLC ϵ acquired filopodia (Fig. 7C, phenotype B) and resembled cells treated with the Ca²⁺ chelator, BAPTA-AM. This phenotype represented about 5% of the population compared with 0% in the absence of PLC ϵ siRNA (phenotype B, Fig. 7D). Additionally, a new phenotype was noted, characterized by the extension of multiple cell protrusions, which represented about 80% of R-Ras^{38V}-expressing cells treated with PLC ϵ siRNA (D in Fig. 7C,D). Overall these data suggest that the effects of R-Ras on the actin cytoskeleton and the formation of the ruffling lamellipod are due in part to PLC ϵ .

Discussion

R-Ras increases integrin-mediated adhesion and many cellular processes that are dependent on integrin function, but the molecular mechanisms involved in these events have remained

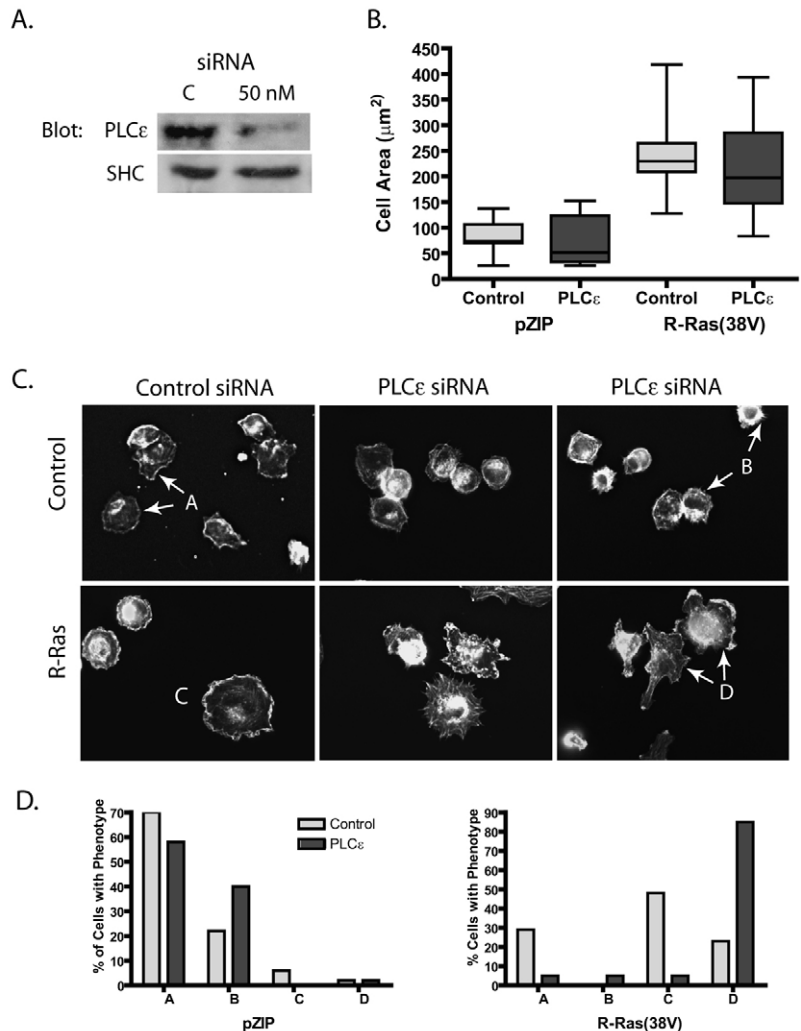


Fig. 7. PLC ϵ mediates R-Ras signaling to membrane protrusions. MCF10A cells stably expressing either a control vector or R-Ras^{38V} were transfected with control siRNA, or 50 nM of pooled siRNA directed against PLC ϵ . (A) Cells were harvested 72 hours later, normalized by cell number and evaluated for PLC ϵ knockdown by immunoblotting with anti-PLC ϵ . (B) PLC ϵ siRNA diminishes the measured area of spreading. Although the effect is not statistically significant, it does extend the mean and range of cell areas measured downward as shown by the box-and-whisker plots. (C) MCF10A cells treated with siRNA against PLC ϵ were allowed to adhere onto 20 μ g/ml fibronectin for 45 minutes, fixed, and then stained with Alexa-phalloidin to evaluate F-actin. Arrows indicate four representative phenotypes (phenotypes A-D) observed and quantified in D. Two different fields for PLC ϵ siRNA to show the range of phenotypes observed. Phenotypes A, B and C are similar to those quantified in Fig. 2. Note the appearance of a new phenotype, D, characterized by multiple membrane protrusions. (D) Quantification of the phenotypes labeled in B for control (pZIP) or R-Ras^{38V}-expressing cells.

elusive. Our data here and previously (Wozniak et al., 2005) demonstrate an important role for R-Ras in the regulation of the actin cytoskeleton and membrane protrusion during both cell spreading and migration. Knocking down endogenous R-Ras by RNAi inhibits membrane protrusion, cell spreading (Fig. 3) and cell migration (Wozniak et al., 2005). Proper regulation of R-Ras activity appears to regulate the actin cytoskeleton and determine the balance between the formation

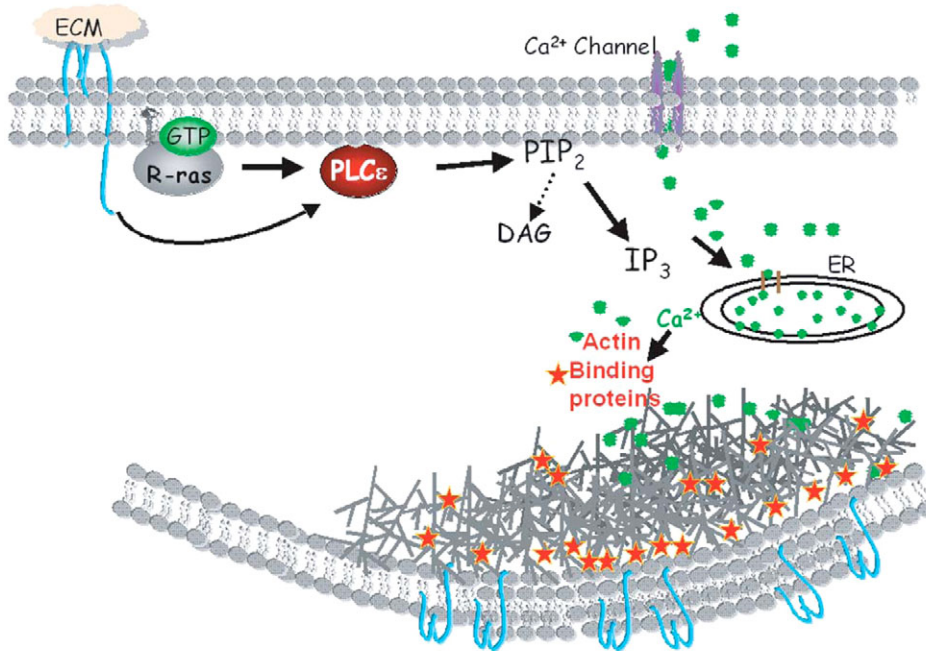


Fig. 8. Proposed signaling pathway by which R-Ras promotes strong lamellipodia formation and cell spreading. We propose that activated R-Ras directly binds to PLC ϵ at the plasma membrane and activates the integrin-PLC- Ca^{2+} -signaling pathway that is required for the initiation of cell protrusion following integrin activation. The stimulation of PLC mobilizes Ca^{2+} from the endoplasmic reticulum. High cytoplasmic Ca^{2+} levels then activate Ca^{2+} -dependent actin-binding proteins, such as capping proteins, causing an increase in actin polymerization. Additionally, Ca^{2+} release may also enhance the recruitment and accumulation of actin and/or adhesion components to the plasma membrane. The overall outcome is the formation of a strong ruffling lamellipod that drives leading-edge protrusion, enhancing cell spreading and adhesion.

of lamellipodia versus filopodia (Fig. 2). Misregulation of R-Ras by the expression of dominant-negative R-Ras^{41A} enhances filopodia formation, whereas expression of constitutively active R-Ras^{38V} inhibits filopodia and results instead in a strong ruffling lamellipod. The formation of this lamellipod in cells expressing constitutively active R-Ras^{38V} increases the persistence of leading-edge protrusion to enhance cell spreading. Further analysis demonstrated that R-Ras regulates the cytoskeleton in part through PLC ϵ (Figs 6 and 7). Inhibiting phospholipase activity by pharmacologic inhibition, siRNA or depleting cytosolic Ca^{2+} with BAPTA abolished the ability of R-Ras cells to form the ruffling lamellipod and diminished cell spreading. Moreover, R-Ras co-immunoprecipitates with a novel isoform of PLC, PLC ϵ and increases its phospholipase activity, suggesting a functional link between R-Ras activation and PLC ϵ .

Based on these results, we propose the following model (Fig. 8): R-Ras is activated by integrin-mediated adhesion (Jeong et al., 2005; Wozniak et al., 2005) and directly binds to and activates PLC ϵ , which in turn, leads to Ca^{2+} mobilization from intracellular stores via IP₃-signaling pathways. The subsequent increase in cytosolic Ca^{2+} concentration locally activates actin-binding proteins, such as capping proteins (Arora et al., 2003; Arora et al., 2004; McGough et al., 2003) and regulates membrane/vesicle trafficking (Bader et al., 2004), all of which will promote the formation of the ruffling lamellipod. The resulting lamellipod exerts outward forces on the plasma membrane leading to an increase in cell spreading. The finding that R-Ras localizes to membrane microdomains (Hansen et al., 2003) and is found on the ruffling lamellipod (Fig. 2) (Kwong, 2003) is consistent with a role in membrane protrusion via PLC ϵ . We further propose that regulation of the actin cytoskeleton and enhanced cell spreading leads to enhanced integrin clustering and adhesion, and the subsequent formation of strong focal adhesions. Indeed, R-Ras enhances focal adhesion formation and integrin-mediated signaling events (Kwong, 2003). Moreover, signaling events leading to

remodeling of the actin cytoskeleton regulate integrin activation and function, presumably in part through the clustering of integrins, which strengthens the adhesion process (Kucik et al., 1996; Lub et al., 1997; Sampath et al., 1998; van Kooyk and Figdor, 2000; Yauch et al., 1997).

Our results suggest that phospholipase C ϵ is a novel effector of R-Ras. R-Ras could be co-precipitated with PLC ϵ under conditions in which a known R-Ras effector, Raf, could also be co-precipitated. When co-expressed in cells, constitutively active R-Ras associated with PLC ϵ to a greater extent than wild-type R-Ras, and activation of R-Ras activated PLC ϵ , both consistent with an effector role for PLC ϵ downstream of R-Ras. Consistent with our findings, it has been previously noted that activated R-Ras2/TC21 also activates PLC ϵ (Kelley et al., 2004). R-Ras was specifically pulled down with the Ras-association domain, RA2, which binds to H-Ras and Rap1 (Kelley et al., 2001; Song et al., 2001). A role for PLC ϵ as an R-Ras effector is further supported by the finding that R-Ras point mutants in the effector-binding loop that eliminate the effects of R-Ras on focal adhesion formation and signaling (Kwong, 2003) are the same point mutations that eliminate H-Ras binding to PLC ϵ (Kelley et al., 2001; Song et al., 2001).

Our results suggest that PLC regulates membrane protrusion and cell spreading. PLC inhibition blocked cell spreading and membrane protrusions in control and R-Ras^{38V}-expressing cells. Our data support recent observations that initiation of protrusion in carcinoma cells is driven by the activation of PLC (Jones et al., 2005; Mounie et al., 2004). Various PLC isoforms have been implicated as key players in early integrin-mediated adhesion (Jones et al., 2005; Keely and Parise, 1996). Our results suggest that the PLC ϵ isoform also regulates early events of spreading and adhesion. Once activated, PLC cleaves phosphoinositol 4,5-bisphosphate (PIP₂). By cleaving PIP₂, PLC activity is thought to decrease membrane tension, allowing the cell to expand its plasma membrane (Raucher and Sheetz, 2000; Raucher and Sheetz, 2001; Raucher et al., 2000). Furthermore, the hydrolysis of PIP₂ relieves the inhibitory

effects of PIP₂ on gelsolin and cofilin, thereby promoting actin polymerization (reviewed by Yin and Janmey, 2003). The cleavage products of PIP₂ – IP₃ and diacylglycerol (DAG) – also have regulatory effects on cell spreading. DAG activates PKC pathways and the MARCKs proteins, all of which have been shown to promote cell spreading (Yue et al., 2000a; Yue et al., 2000b; Zhou and Li, 2000). Previously we have shown that PKC pathways were partially involved in the promotion of haptotactic migration by R-Ras^{38V} (Keely et al., 1999).

IP₃, on the other hand, mobilizes internal Ca²⁺ stores. Recently, Itano et al. showed that endoplasmic and nuclear Ca²⁺ stores are released during cell spreading (Itano et al., 2003). Moreover, thapsagargin treatment to release Ca²⁺ stores enhances the formation of lamellipodia in epithelial cells (Price et al., 2003). ER Ca²⁺ levels are misregulated in cells overexpressing R-Ras^{38V} (Fig. 5C) (Koopman et al., 2003), suggesting that R-Ras activation does indeed cause the release of Ca²⁺ from ER stores. This rise in intracellular Ca²⁺ is necessary for R-Ras to induce the ruffling lamellipod, as formation of the lamellipod was inhibited by cells treated with the intracellular Ca²⁺ chelator, BAPTA-AM (Fig. 5A). We propose that the resulting rise in Ca²⁺ concentration activates Ca²⁺-dependent actin-remodeling proteins, such as gelsolin and other capping proteins (Lader et al., 1999; Lin et al., 2000; Sun et al., 1999). Indeed, we find that formation of the ruffling lamellipod observed in R-Ras^{38V}-expressing cells depends on the activity of gelsolin (A.S.A.-N. and P.J.K., unpublished data).

The cAMP-Epac-Rap pathway has been shown to directly activate PLC ϵ to mobilize intracellular Ca²⁺ and promote cell adhesion (Jin et al., 2001; Rangarajan et al., 2003; Schmidt et al., 2001; Song et al., 2002; Stope et al., 2004). Recently, R-Ras was also shown to be activated by cAMP (Cole et al., 2003) (A.S.A.-N. and P.J.K., unpublished results), suggesting that it may be in this cAMP-Epac pathway. In addition to Ras-association domains, PLC ϵ contains a Cdc25 domain that functions as an exchange factor for H-Ras and Rap1 (Jin et al., 2001; Lopez et al., 2001). Whether PLC ϵ is not only an effector, but also an exchange factor for R-Ras, and mediates R-Ras activation by cAMP remains to be determined. However, PLC ϵ could serve as an exchange factor by which R-Ras activates Rap1, as some of the effects of R-Ras on adhesion and phagocytosis are dependent on Rap1 (Bos et al., 2003; Caron et al., 2000; Ohba et al., 2001; Self et al., 2001; Song et al., 2001; Song et al., 2002). In light of this new evidence, we propose that R-Ras1, R-Ras2 and Rap1 have redundant functions in the regulation of integrin signaling through the activation of a common PLC ϵ -Ca²⁺-integrin pathway.

Membrane protrusion is driven by actin polymerization, myosin-based retractions and actin depolymerization events. Whether protrusion takes the form of filopodia, lamellipodia or both is regulated by several actin binding proteins including capping protein, ADF/cofilin, WASp/Scar proteins, Mena/VASP, and Arp2/3, which determine the degree of branching of the actin network (Bear et al., 2002; Mallavarapu and Mitchison, 1999; Mejillano et al., 2004; Pollard and Borisy, 2003; Small et al., 2002; Vignjevic et al., 2003). TIRF analysis shows that R-Ras^{38V} cells exhibit long-lived extension events and minimal retraction events to yield robust spreading and a significant increase in cell surface area. Exactly how R-

Ras^{38V} signaling opposes the retraction events is not clear at this moment. Our data show that actin polymerization is greatly enhanced in R-Ras^{38V} cells, as shown by the ruffling lamellipod (Fig. 3A) and by biochemical analysis demonstrating a substantial increase in the insoluble actin fraction (A.S.A.-N. and P.J.K., unpublished data). Moreover, many actin-binding proteins involved in protrusive extensions were enhanced in the actin insoluble fraction and exhibited strong colocalization with F-actin at the protruding lamellipod (A.S.A.-N. and P.J.K., unpublished data).

Recent reports (Jeong et al., 2005; Wozniak et al., 2005) demonstrate that the activation of R-Ras inhibits membrane protrusion during cell migration, whereas here we report that R-Ras activation enhances protrusion during cell spreading (Fig. 1), but inhibits random cell migration (Movies 1-4 in supplementary material). Thus, there appears to be a difference in the mechanism of cell spreading versus cell migration. During cell spreading, R-Ras enhances leading-edge protrusions that lead to enhanced adhesion. Once a cell has become stably attached, this enhanced adhesion could prevent further protrusions (Cox et al., 2001). For cell migration, cells require short-lived extension and retraction events, which result in a net movement of the leading and trailing edge of the cell (Dunn et al., 1997). The inability of R-Ras^{38V} cells to move suggests that misregulating membrane protrusions in any way would hamper the ability of these cells to migrate. Cell migration is dependent on the ability of a cell to polarize and provide directionality to membrane protrusions. Misregulation of R-Ras by expression of R-Ras^{38V} eliminates cell polarity (Fig. 3) (Wozniak et al., 2005), which is needed for cell migration, but apparently not for cell spreading.

Our data suggest that the effects of R-Ras^{38V} on cell adhesion and focal adhesion formation occur secondarily to its effects on membrane protrusion during cell spreading. Focal adhesion formation does not occur until well after the cells have spread, consistent with the idea that a cell must achieve a given size in order to generate the internal forces necessary for focal adhesion formation (Chen et al., 2003; Tan et al., 2003). In support of this, we find that inhibitors of Rho/ROCK contractility block the formation of large focal adhesions (Wozniak et al., 2005), but have no effect on the spreading and formation of the dense actin network noted here (data not shown), consistent with the idea that focal adhesion formation is subsequent to cell spreading. Therefore, the combined effects of R-Ras on increasing cell-ECM contact area through cell spreading, and regulating the organization of the actin cytoskeleton probably contribute to an increase in integrin avidity and cell adhesion.

The formation of the lamellipodia in R-Ras^{38V} cells was not associated with an increase in Rac activation, nor was it mediated by PI3K (our unpublished observations). Thus, our work hints at a novel Rac-independent pathway in the regulation of lamellipodia formation that instead involves R-Ras proteins. So far, Rab5, a small G-protein involved in the regulation of vesicle fusion and trafficking, has been shown to induce lamellipodia in a PI3K-Rac independent manner (Spaargaren et al., 1994). The novel mechanism mediated by Rab5 was strongly correlated to its ability to promote endocytosis. Whether R-Ras could regulate vesicle trafficking is unclear at this point, but the strong ruffles suggest that this is a possibility.

In summary, R-Ras is an important regulator of membrane protrusion and the actin cytoskeleton during both cell spreading and cell migration. Enhanced cell spreading is driven by the formation of a strong ruffling lamellipod due in part to the action of PLC ϵ and the release of intracellular Ca $^{2+}$ downstream of R-Ras signaling. Moreover, misregulation of R-Ras disrupts cell polarity and migration, suggesting that R-Ras-mediated activation of PLC pathways is normally regulated in a spatial and temporal manner.

Materials and Methods

MCF10A cell lines

MCF10A cells were infected with pZIP retrovirus or pZIP containing R-Ras in which glycine 38 was mutated to valine (R-Ras 38V), and selected in G418 as pools of stable transfectants using protocols previously described (Clark et al., 1996). Expression of R-Ras 38V was verified by immunoblotting using anti-R-Ras antibody (Santa Cruz Biochemicals, Santa Cruz, CA).

Total internal fluorescence microscopy and adhesion assay

Cells in suspension were loaded with 5 μ M calcein-AM (Molecular Probes) for 20 minutes and centrifuged at low velocity. Cells were imaged with a 20 \times water-immersion objective for calcein using an upright Olympus BX-50 microscope using 568 nm fluorescent excitation light from a Melles Griot krypton-ion laser. Images were recorded with a Coolsnap FX CCD camera. Individual fluorescent TIRF images of spreading cells were processed as described elsewhere using a custom MATLAB program in which the outer cell perimeter was fitted with a contour (Dubin-Thaler et al., 2004; Giannone et al., 2004). Further analysis was performed as described (Dubin-Thaler et al., 2004). For the adhesion assay, control and R-Ras 38V cells were loaded with 20 μ g/ml Calcein-AM for 20 minutes, centrifuged and resuspended in medium pretreated with the indicated pharmacological agent (DMSO, EGTA, BAPTA and U73122 PLC inhibitor) for 30 minutes, followed by adhesion on 96-well plates coated with 20 μ g/ml fibronectin for 15 or 50 minutes. Cells were washed three times with PBS and adherent cells were evaluated with a fluorescent plate reader.

Cell stimulation and immunofluorescence microscopy

MCF10A cells were detached from tissue-culture flasks using 1 mg/ml TPCK trypsin (Sigma). Trypsin was inactivated using 1 mg/ml soy bean trypsin inhibitor (Sigma), and washed into serum-free DMEM F12 media supplemented with 5 mg/ml fatty-acid-free BSA for about 20 minutes. If treated with inhibitors [LY294002 (Alexis Biochemicals), BAPTA-AM (Molecular probes), U73122 (Sigma), EGTA (Sigma)], cells were pretreated with inhibitor for 20-30 minutes at 37°C in suspension. Cells were then plated on plastic dishes or glass coverslips coated with 30 μ g/ml collagen I (BD Bioscience), 20 μ g/ml human fibronectin (BD Bioscience), or 0.01% poly-L-lysine (Sigma) for the indicated time points. Following adhesion, cells were rinsed with PBS and fixed for 15 minutes in 4% paraformaldehyde at room temperature. Formaldehyde was quenched with 0.15 M glycine in PBS. Cells were permeabilized with 0.2% Triton X-100 in PBS, blocked with 1% donkey serum (Jackson ImmunoResearch) and BSA (Fisher Scientific) in PBS and detected with the antibodies of interest. Coverslips were mounted using Prolong antifade mounting medium (Molecular Probes). Microscopy was performed using a Nikon Eclipse TE300 inverted microscope with a Coolsnap FX CCD camera (Roper Scientific). Images were collected and three-dimensional (3D) deconvolution was performed using Inovision software (Durham, NC). Time-lapse images were acquired with E-See Inovision Software (Inovision, Raleigh, NC) as previously described (Wozniak et al., 2005), with one image taken every 60 seconds for 100 minutes.

Measurement of cell areas

Digital photographs were captured for random fields from each experiment, and the area of 20 or more individual cells was quantified by tracing the perimeter of the cell, and using Image J software to calculate area, perimeter, and circularity. Data for cell area was further analyzed using GraphPad Prism version 4.00 for Windows (GraphPad Software, San Diego, CA) to perform statistical analysis using two-tailed unpaired *t*-tests.

Cell transfection

MCF10A cells were seeded into 12-well plates and grown and maintained at 37°C in 10% CO $_2$ atmosphere in DMEM/F-12 medium containing 5% horse serum. Cells were transfected with dominant-negative R-Ras construct (R-Ras 41A) in a pCMV5 vector and GFP vector (green lantern) using Mirus TransIT-LT1 transfection reagent. 48 hours post transfection, cells were detached and cell spreading assays performed on fibronectin coated coverslips. MCF10A cells were seeded into six-well plates and grown and maintained at 37°C in a 10% CO $_2$ atmosphere in DMEM/F-12 medium containing 5% horse serum. Cells were transfected with a pool of three PLC ϵ siRNAs

from Ambion (GCA-CAU-ACU-GUC-AGA-CGA-Att and UUC-GUC-UGA-CAG-UAU-GUG-Ctt; GGU-GAU-AGC-UUU-UGU-AGG-Att and UCC-UAC-AAA-AGC-UAU-CAC-Ctg; GGG-ACU-AAU-AAU-GUC-AUU-UGA-Att and UUC-AAA-UGA-CAU-UAG-UCC-Ctg) using siQuest reagent (Mirus). 72 hours post transfection, cells were lysed and PLC ϵ protein levels were assessed by western blotting and fluorescence microscopy using an unpurified anti-PLC ϵ antibody (Kelley et al., 2004). For siRNA approaches, MCF10A cells were transfected with siRNA directed against R-Ras or against PLC ϵ (each designed as a pool obtained from Dharmacon) using siQuest reagent (Mirus). T47D cells were transfected with siRNA directed against R-Ras as previously described (Wozniak et al., 2005).

Co-immunoprecipitation, immunoblotting, pulldown and cell fractionation

Cos7 cells were transiently transfected with pCMV-PLC ϵ , pCMV-R-Ras and pCMV-R-Ras 38V constructs lysed in ice-cold modified RIPA buffer containing 1% NP-40 or 1% Triton X-100 (Keely and Parise, 1996; Keely et al., 1999). PLC ϵ was immunoprecipitated by incubating Flag antibody and gamma Sepharose beads with a clarified cell lysate overnight while rotating at 4°C. Immunoprecipitates were separated on acrylamide gels, transferred to PVDF membrane and immunoblotted with the appropriate antibodies. For whole-cell lysate analysis, cells were stimulated by adhesion on fibronectin and lysed with SDS-Laemmli buffer. Lysates were separated on acrylamide gels, transferred to PVDF membrane and immunoblotted with the appropriate antibodies. To measure Cdc42 and Rac activation, cells were stimulated by adhesion on fibronectin (20 μ g/ml) and collagen I (30 μ g/ml) for the indicated time. Cells were lysed in a modified RIPA buffer containing 1% Nonidet P-40 (MP Biomedicals). After centrifugation, supernatant was incubated with Raf-RBD coupled to glutathione-Sepharose beads. Bound Rac and Cdc42 were detected by immunoblotting with respective antibodies (Transduction Labs). To measure R-Ras and PLC ϵ interaction, cells were stimulated by adhesion on fibronectin (20 μ g/ml) for 45 minutes and 8-CPT-2Me-cAMP (200 μ M) for 30 minutes. Cells were lysed in ice-cold modified RIPA buffer containing 1% Nonidet P-40 (MP Biomedicals) or 1% Triton X-100 (Keely et al., 1999). After centrifugation, the clarified lysate was incubated with GST, GST-Raf-RBD and GST-RA2 (Kelley et al., 2001; Kelley et al., 2004) for 2 hours while rotating at 4°C. Bound R-Ras was detected on immunoblot with an anti-R-Ras antibody (BD-Bioscience-Pharmingen).

Phospholipase C assay

Cos7 cells were seeded on six-well plates and transfected with 3 μ g plasmid encoding PLC ϵ (Song et al., 2001) and 1 μ g of dominant-negative R-Ras (R-Ras 41A) or activated R-Ras (R-Ras 38V), using Mirus TransIT-LT1 transfection reagent (Mirus). For PLC assay measurements (Kelley et al., 2001; Kelley et al., 2004), 24 hours post-transfection, Cos7 cells were labeled with 4 μ Ci myo-D-[2-3H]-inositol (Perkin-Elmer) in inositol- and serum-free Dulbecco's modified Eagle's medium for 24 hours. Cell labeling with myo-D-[2-3H]-inositol was stopped by removing the incubation medium and quenching cells with 1.5 ml of 60 mM perchloric acid plus 0.2 mg/ml InsP6 on ice for 30 minutes. The acidified supernatant was transferred to a polypropylene tube and neutralized with 650 μ l of 1M K $_2$ CO $_3$ plus 5 mM EDTA. The samples were kept on ice overnight. Total inositol phosphates were purified by gravity-fed column chromatography using AG 1-X8 200-400 μ m mesh, formate form (Bio-Rad), and quantified by liquid scintillation counting (Shears, 1997). The expression of R-Ras and PLC constructs were determined in parallel plates without radioactivity by western blotting and were not significantly different within each experiment (Clark et al., 1996).

Ca $^{2+}$ flux

MCF10A cells were detached with TPCK trypsin (1 mg/ml in PBS (Sigma, St Louis, MO). Trypsin was neutralized with soy bean trypsin inhibitor (1 mg/ml in PBS) (Sigma) and loaded with 2 μ g/ml of indo1-AM (Molecular Probes) for 20 minutes at 37°C with occasional shaking. Intracellular Ca $^{2+}$ concentrations were determined by flow cytometry following stimulation for 6-10 minutes with 4 μ M thapsigargin (Sigma), 1 μ M CaCl $_2$ or 60 μ M ionomycin (Calbiochem).

The authors thank Grant Kelley for providing antibodies and reagents for PLC ϵ , David Inman for expert technical assistance, Chunhua Song for helpful discussion, and Erik Peden, Scott Gehler and Matt Conklin for comments on the manuscript. This work was supported by grants from the NIH/NCI (CA076537) and the Milwaukee Research Foundation (both to P.J.K.).

References

- Arora, P. D., Fan, L., Sodek, J., Kapus, A. and McCulloch, C. A. (2003). Differential binding to dorsal and ventral cell surfaces of fibroblasts: effect on collagen phagocytosis. *Exp. Cell Res.* **286**, 366-380.
- Arora, P. D., Glogauer, M., Kapus, A., Kwiatkowski, D. J. and McCulloch, C. A. (2004). Gelsolin mediates collagen phagocytosis through a rac-dependent step. *Mol. Biol. Cell* **15**, 588-599.

- Bader, M. F., Doussau, F., Chasserot-Golaz, S., Vitale, N. and Gasman, S. (2004). Coupling actin and membrane dynamics during calcium-regulated exocytosis: a role for Rho and ARF GTPases. *Biochim. Biophys. Acta* **1742**, 37-49.
- Bailly, M., Yan, L., Whitesides, G. M., Condeelis, J. S. and Segall, J. E. (1998). Regulation of protrusion shape and adhesion to the substratum during chemotactic responses of mammalian carcinoma cells. *Exp. Cell Res.* **241**, 285-299.
- Bear, J. E., Svitkina, T. M., Krause, M., Schafer, D. A., Loureiro, J. J., Strasser, G. A., Maly, I. V., Chaga, O. Y., Cooper, J. A., Borisy, G. G. et al. (2002). Antagonism between Ena/VASP proteins and actin filament capping regulates fibroblast motility. *Cell* **109**, 509-521.
- Berrier, A. L., Mastrangelo, A. M., Downward, J., Ginsberg, M. and LaFlamme, S. E. (2000). Activated R-ras, Rac1, PI 3-kinase and PKCepsilon can each restore cell spreading inhibited by isolated integrin beta1 cytoplasmic domains. *J. Cell Biol.* **151**, 1549-1560.
- Bos, J. L., de Bruyn, K., Enserink, J., Kuiperij, B., Rangarajan, S., Rehmann, H., Riedl, J., de Rooij, J., van Mansfeld, F. and Zwartkruis, F. (2003). The role of Rap1 in integrin-mediated cell adhesion. *Biochem. Soc. Trans.* **31**, 83-86.
- Caron, E., Self, A. J. and Hall, A. (2000). The GTPase Rap1 controls functional activation of macrophage integrin alphaMbeta2 by LPS and other inflammatory mediators. *Curr. Biol.* **10**, 974-978.
- Chen, C. S., Alonso, J. L., Ostuni, E., Whitesides, G. M. and Ingber, D. E. (2003). Cell shape provides global control of focal adhesion assembly. *Biochem. Biophys. Res. Commun.* **307**, 355-361.
- Clark, G. J., Kinch, M. S., Gilmer, T. M., Burrridge, K. and Der, C. J. (1996). Overexpression of the Ras-related TC21/R-Ras2 protein may contribute to the development of human breast cancers. *Oncogene* **12**, 169-176.
- Cole, A. L., Subbanagounder, G., Mukhopadhyay, S., Berliner, J. A. and Vora, D. K. (2003). Oxidized phospholipid-induced endothelial cell/monocyte interaction is mediated by a cAMP-dependent R-Ras/PI3-kinase pathway. *Arterioscler. Thromb. Vasc. Biol.* **23**, 1384-1390.
- Cox, E. A., Sastry, S. K. and Huttenlocher, A. (2001). Integrin-mediated adhesion regulates cell polarity and membrane protrusion through the Rho family of GTPases. *Mol. Biol. Cell* **12**, 265-277.
- Czyzyk, J., Brogdon, J. L., Badou, A., Henegariu, O., Preston Hurlburt, P., Flavell, R. and Bottomly, K. (2003). Activation of CD4 T cells by Raf-independent effectors of Ras. *Proc. Natl. Acad. Sci. USA* **100**, 6003-6008.
- Dubin-Thaler, B. J., Giannone, G., Dobreiner, H. G. and Sheetz, M. P. (2004). Nanometer analysis of cell spreading on matrix-coated surfaces reveals two distinct cell states and STEPs. *Biophys. J.* **86**, 1794-1806.
- Dunn, G. A., Zicha, D. and Fraylich, P. E. (1997). Rapid, microtubule-dependent fluctuations of the cell margin. *J. Cell Sci.* **110**, 3091-3098.
- Engler, A., Bacakova, L., Newman, C., Hategan, A., Griffin, M. and Discher, D. (2004). Substrate compliance versus ligand density in cell on gel responses. *Biophys. J.* **86**, 617-628.
- Giannone, G., Dubin-Thaler, B. J., Dobreiner, H. G., Kieffer, N., Bresnick, A. R. and Sheetz, M. P. (2004). Periodic lamellipodial contractions correlate with rearward actin waves. *Cell* **116**, 431-443.
- Hansen, M., Prior, I. A., Hughes, P. E., Oertli, B., Chou, F. L., Willumsen, B. M., Hancock, J. F. and Ginsberg, M. H. (2003). C-terminal sequences in R-Ras are involved in integrin regulation and in plasma membrane microdomain distribution. *Biochem. Biophys. Res. Commun.* **311**, 829-838.
- Itano, N., Okamoto, S., Zhang, D., Lipton, S. A. and Ruoslahti, E. (2003). Cell spreading controls endoplasmic and nuclear calcium: a physical gene regulation pathway from the cell surface to the nucleus. *Proc. Natl. Acad. Sci. USA* **100**, 5181-5186.
- Ivins, J. K., Yurchenco, P. D. and Lander, A. D. (2000). Regulation of neurite outgrowth by integrin activation. *J. Neurosci.* **20**, 6551-6560.
- Jeong, H. W., Nam, J. O. and Kim, I. S. (2005). The COOH-terminal end of R-Ras alters the motility and morphology of breast epithelial cells through Rho/Rho-kinase. *Cancer Res.* **65**, 507-515.
- Jin, T. G., Satoh, T., Liao, Y., Song, C., Gao, X., Kariya, K., Hu, C. D. and Kataoka, T. (2001). Role of the CDC25 homology domain of phospholipase Cepsilon in amplification of Rap1-dependent signaling. *J. Biol. Chem.* **276**, 30301-30307.
- Jones, N. P., Peak, J., Brader, S., Eccles, S. A. and Katan, M. (2005). PLCgamma1 is essential for early events in integrin signalling required for cell motility. *J. Cell Sci.* **118**, 2695-2706.
- Jones, S. L., Wang, J., Turck, C. W. and Brown, E. J. (1998). A role for the actin-binding protein L-plastin in the regulation of leukocyte integrin function. *Proc. Natl. Acad. Sci. USA* **95**, 9331-9336.
- Keely, P. and Parise, L. (1996). The alpha2beta1 integrin is a necessary co-receptor for collagen-induced activation of Syk and the subsequent phosphorylation of phospholipase Cgamma2 in platelets. *J. Biol. Chem.* **271**, 26668-26676.
- Keely, P. J., Rusyn, E. V., Cox, A. D. and Parise, L. V. (1999). R-Ras signals through specific integrin alpha cytoplasmic domains to promote migration and invasion of breast epithelial cells. *J. Cell Biol.* **145**, 1077-1088.
- Kelley, G. G., Reks, S. E., Ondrako, J. M. and Smrcka, A. V. (2001). Phospholipase C(epsilon): a novel Ras effector. *EMBO J.* **20**, 743-754.
- Kelley, G. G., Reks, S. E. and Smrcka, A. V. (2004). Hormonal regulation of phospholipase Cepsilon through distinct and overlapping pathways involving G12 and Ras family G-proteins. *Biochem. J.* **378**, 129-139.
- Koopman, W. J., Bosch, R. R., van Ernst-de Vries, S. E., Spaargaren, M., De Pont, J. J. and Willems, P. H. (2003). R-Ras alters Ca²⁺ homeostasis by increasing the Ca²⁺ leak across the endoplasmic reticular membrane. *J. Biol. Chem.* **278**, 13672-13679.
- Kucik, D. F., Dustin, M. L., Miller, J. M. and Brown, E. J. (1996). Adhesion-activating phorbol ester increases the mobility of leukocyte integrin LFA-1 in cultured lymphocytes. *J. Clin. Invest.* **97**, 2139-2144.
- Kwong, L., Wozniak, M., Collins, A. S., Wilson, S. D. and Keely, P. J. (2003). R-Ras promotes focal adhesion formation through focal adhesion kinase and p130cas by a novel mechanism that differs from integrins. *Mol. Cell Biol.* **23**, 933-949.
- Lader, A. S., Kwiatkowski, D. J. and Cantiello, H. F. (1999). Role of gelsolin in the actin filament regulation of cardiac L-type calcium channels. *Am. J. Physiol.* **277**, C1277-C1283.
- Lin, K. M., Mejillano, M. and Yin, H. L. (2000). Ca²⁺ regulation of gelsolin by its C-terminal tail. *J. Biol. Chem.* **275**, 27746-27752.
- Lopez, L., Mak, E. C., Ding, J., Hamm, H. E. and Lomasney, J. W. (2001). A novel bifunctional phospholipase c that is regulated by Galpha 12 and stimulates the Ras/mitogen-activated protein kinase pathway. *J. Biol. Chem.* **276**, 2758-2765.
- Lub, M., van Kooyk, Y., van Vliet, S. J. and Figdor, C. G. (1997). Dual role of the actin cytoskeleton in regulating cell adhesion mediated by the integrin lymphocyte function-associated molecule-1. *Mol. Biol. Cell* **8**, 341-351.
- Mallavarapu, A. and Mitchison, T. (1999). Regulated actin cytoskeleton assembly at filopodium tips controls their extension and retraction. *J. Cell Biol.* **146**, 1097-1106.
- McGough, A. M., Staiger, C. J., Min, J. K. and Simonetti, K. D. (2003). The gelsolin family of actin regulatory proteins: modular structures, versatile functions. *FEBS Lett.* **552**, 75-81.
- McNamee, H. P., Ingber, D. E. and Schwartz, M. A. (1993). Adhesion to fibronectin stimulates inositol lipid synthesis and enhances PDGF-induced inositol lipid breakdown. *J. Cell Biol.* **121**, 673-678.
- McNamee, H. P., Liley, H. G. and Ingber, D. E. (1996). Integrin-dependent control of inositol lipid synthesis in vascular endothelial cells and smooth muscle cells. *Exp. Cell Res.* **224**, 116-122.
- Mejillano, M. R., Kojima, S., Applewhite, D. A., Gertler, F. B., Svitkina, T. M. and Borisy, G. G. (2004). Lamellipodial versus filopodial mode of the actin nanomachinery: pivotal role of the filament barbed end. *Cell* **118**, 363-373.
- Mouneimne, G., Soon, L., DesMarais, V., Sidani, M., Song, X., Yip, S. C., Ghosh, M., Eddy, R., Backer, J. M. and Condeelis, J. (2004). Phospholipase C and cofilin are required for carcinoma cell directionality in response to EGF stimulation. *J. Cell Biol.* **166**, 697-708.
- Ohba, Y., Ikuta, K., Ogura, A., Matsuda, J., Mochizuki, N., Nagashima, K., Kurokawa, K., Mayer, B. J., Maki, K., Miyazaki, J. et al. (2001). Requirement for C3G-dependent Rap1 activation for cell adhesion and embryogenesis. *EMBO J.* **20**, 3333-3341.
- Pantaloni, D., Le Clairche, C. and Carlier, M. F. (2001). Mechanism of actin-based motility. *Science* **292**, 1502-1506.
- Parekh, A. B. (2003). Store-operated Ca²⁺ entry: dynamic interplay between endoplasmic reticulum, mitochondria and plasma membrane. *J. Physiol.* **547**, 333-348.
- Pettit, E. J. and Hallett, M. B. (1996a). Integrin triggered Ca²⁺ signalling in human neutrophils. *Biochem. Soc. Trans.* **24**, 70S.
- Pettit, E. J. and Hallett, M. B. (1996b). Localised and global cytosolic Ca²⁺ changes in neutrophils during engagement of Cd11b/CD18 integrin visualised using confocal laser scanning reconstruction. *J. Cell Sci.* **109**, 1689-1694.
- Pettit, E. J. and Hallett, M. B. (1998). Release of 'caged' cytosolic Ca²⁺ triggers rapid spreading of human neutrophils adherent via integrin engagement. *J. Cell Sci.* **111**, 2209-2215.
- Pollard, T. D. and Borisy, G. G. (2003). Cellular motility driven by assembly and disassembly of actin filaments. *Cell* **112**, 453-465.
- Price, L. S., Langeslag, M., Klooster, J. P. t., Horstrijk, P. L., Jalink, K. and Collard, J. G. (2003). Calcium signaling regulates translocation and activation of rac. *J. Biol. Chem.* **278**, 39413-39421.
- Rangarajan, S., Enserink, J. M., Kuiperij, H. B., de Rooij, J., Price, L. S., Schwede, F. and Bos, J. L. (2003). Cyclic AMP induces integrin-mediated cell adhesion through Epac and Rap1 upon stimulation of the beta 2-adrenergic receptor. *J. Cell Biol.* **160**, 487-493.
- Raucher, D. and Sheetz, M. P. (2000). Cell spreading and lamellipodial extension rate is regulated by membrane tension. *J. Cell Biol.* **148**, 127-136.
- Raucher, D. and Sheetz, M. P. (2001). Phospholipase C activation by anesthetics decreases membrane-cytoskeleton adhesion. *J. Cell Sci.* **114**, 3759-3766.
- Raucher, D., Stauffer, T., Chen, W., Shen, K., Guo, S., York, J. D., Sheetz, M. P. and Meyer, T. (2000). Phosphatidylinositol 4,5-bisphosphate functions as a second messenger that regulates cytoskeleton-plasma membrane adhesion. *Cell* **100**, 221-228.
- Sampath, R., Gallagher, P. J. and Pavalko, F. M. (1998). Cytoskeletal interactions with the leukocyte integrin beta2 cytoplasmic tail. Activation-dependent regulation of associations with talin and alpha-actinin. *J. Biol. Chem.* **273**, 33588-33594.
- Schmidt, M., Evellin, S., Weernink, P. A., von Dorp, F., Rehmann, H., Lomasney, J. W. and Jakobs, K. H. (2001). A new phospholipase-C-calcium signalling pathway mediated by cyclic AMP and a Rap GTPase. *Nat. Cell Biol.* **3**, 1020-1024.
- Sechi, A. S. and Wehland, J. (2000). The actin cytoskeleton and plasma membrane connection: PtdIns(4,5)P(2) influences cytoskeletal protein activity at the plasma membrane. *J. Cell Sci.* **113**, 3685-3695.
- Self, A. J., Caron, E., Paterson, H. F. and Hall, A. (2001). Analysis of R-Ras signalling pathways. *J. Cell Sci.* **114**, 1357-1366.
- Sethi, T., Ginsberg, M. H., Downward, J. and Hughes, P. E. (1999). The small GTP-binding protein R-Ras can influence integrin activation by antagonizing a Ras/Raf-initiated integrin suppression pathway. *Mol. Biol. Cell* **10**, 1799-1809.
- Shears, S. (1997). Measurement of inositol phosphate turnover in intact cells and cell-

- free systems. In *Signalling by Inositides* (ed. S. Shears), pp. 33. Oxford, New York: IRL Press at Oxford University Press.
- Small, J. V., Stradal, T., Vignat, E. and Rottner, K.** (2002). The lamellipodium: where motility begins. *Trends Cell Biol.* **12**, 112-120.
- Song, C., Hu, C. D., Masago, M., Kariyai, K., Yamawaki-Kataoka, Y., Shibatohe, M., Wu, D., Satoh, T. and Kataoka, T.** (2001). Regulation of a novel human phospholipase C, PLCepsilon, through membrane targeting by Ras. *J. Biol. Chem.* **276**, 2752-2757.
- Song, C., Satoh, T., Edamatsu, H., Wu, D., Tadano, M., Gao, X. and Kataoka, T.** (2002). Differential roles of Ras and Rap1 in growth factor-dependent activation of phospholipase C epsilon. *Oncogene* **21**, 8105-8113.
- Spaargaren, M., Martin, G. A., McCormick, F., Fernandez-Sarabia, M. J. and Bischoff, J. R.** (1994). The Ras-related protein R-ras interacts directly with Raf-1 in a GTP-dependent manner. *Biochem. J.* **300**, 303-307.
- Spoonster, J. R., Masiero, L., Savage, S. A., Probst, J. and Kohn, E. C.** (1997). Regulation of cell spreading during differentiation in the muscarinic M5 receptor tumor-suppressor model. *Int. J. Cancer* **72**, 362-368.
- Stope, M. B., Vom Dorp, F., Szatkowski, D., Bohm, A., Keiper, M., Nolte, J., Oude Weernink, P. A., Rosskopf, D., Evellin, S., Jakobs, K. H. et al.** (2004). Rap2B-dependent stimulation of phospholipase C-epsilon by epidermal growth factor receptor mediated by c-Src phosphorylation of RasGRP3. *Mol. Cell Biol.* **24**, 4664-4676.
- Sun, H. Q., Yamamoto, M., Mejillano, M. and Yin, H. L.** (1999). Gelsolin, a multifunctional actin regulatory protein. *J. Biol. Chem.* **274**, 33179-33182.
- Svitkina, T. M., Bulanova, E. A., Chaga, O. Y., Vignjevic, D. M., Kojima, S., Vasiliev, J. M. and Borisy, G. G.** (2003). Mechanism of filopodia initiation by reorganization of a dendritic network. *J. Cell Biol.* **160**, 409-421.
- Takenawa, T. and Itoh, T.** (2001). Phosphoinositides, key molecules for regulation of actin cytoskeletal organization and membrane traffic from the plasma membrane. *Biochim. Biophys. Acta* **1533**, 190-206.
- Tan, J. L., Tien, J., Pirone, D. M., Gray, D. S., Bhadriraju, K. and Chen, C. S.** (2003). Cells lying on a bed of microneedles: an approach to isolate mechanical force. *Proc. Natl. Acad. Sci. USA* **100**, 1484-1489.
- van Kooyk, Y. and Figdor, C. G.** (2000). Avidity regulation of integrins: the driving force in leukocyte adhesion. *Curr. Opin. Cell Biol.* **12**, 542-547.
- van Kooyk, Y., van Vliet, S. J. and Figdor, C. G.** (1999). The actin cytoskeleton regulates LFA-1 ligand binding through avidity rather than affinity changes. *J. Biol. Chem.* **274**, 26869-26877.
- Vignjevic, D., Yarar, D., Welch, M. D., Peloquin, J., Svitkina, T. and Borisy, G. G.** (2003). Formation of filopodia-like bundles in vitro from a dendritic network. *J. Cell Biol.* **160**, 951-962.
- Wakatsuki, T., Schwab, B., Thompson, N. C. and Elson, E. L.** (2001). Effects of cytochalasin D and latrunculin B on mechanical properties of cells. *J. Cell Sci.* **114**, 1025-1036.
- Wozniak, M. A., Kwong, L., Chodniewicz, D., Klemke, R. L. and Keely, P. J.** (2005). R-Ras controls membrane protrusion and cell migration through the spatial regulation of Rac and Rho. *Mol. Biol. Cell* **16**, 84-96.
- Yauch, R. L., Felsenfeld, D. P., Kraeft, S. K., Chen, L. B., Sheetz, M. P. and Hemler, M. E.** (1997). Mutational evidence for control of cell adhesion through integrin diffusion/clustering, independent of ligand binding. *J. Exp. Med.* **186**, 1347-1355.
- Yin, H. L. and Janmey, P. A.** (2003). Phosphoinositide regulation of the actin cytoskeleton. *Annu. Rev. Physiol.* **65**, 761-789.
- Yue, L., Bao, Z. and Li, J.** (2000a). Expression of MacMARCKS restores cell adhesion to ICAM-1-coated surface. *Cell Adhes. Commun.* **7**, 359-366.
- Yue, L., Lu, S., Garces, J., Jin, T. and Li, J.** (2000b). Protein kinase C-regulated dynamin-macrophage-enriched myristoylated alanine-rich C kinase substrate interaction is involved in macrophage cell spreading. *J. Biol. Chem.* **275**, 23948-23956.
- Zhang, Z., Vuori, K., Wang, H., Reed, J. C. and Ruoslahti, E.** (1996). Integrin activation by R-ras. *Cell* **85**, 61-69.
- Zhou, X. and Li, J.** (2000). Macrophage-enriched myristoylated alanine-rich C kinase substrate and its phosphorylation is required for the phorbol ester-stimulated diffusion of beta 2 integrin molecules. *J. Biol. Chem.* **275**, 20217-20222.